F. VODOPIVEC, B. ARZENŠEK, J. VOJVODIČ TUMA, R. CELIN

ISSN 0543-5846
METABK 47(3) 173-179 (2008)
UDC – UDK 624.94:621.974:620.19=111

THE CHARPY FRACTURING PROCESS IN DUCTILE RANGE

Received – Prispjelo: 2007-08-31
Accepted – Prihvaćeno: 2008-01-30
Original Scientific Paper – Izvorni znanstveni rad

The fracturing of structural steels in Charpy ductile range is investigated. The dependences load versus deflection and time were recorded and the consumption of energy for different fracturing events, as f.i. plastic deflection and crack propagation was assessed. The micromorphology of the crack surface and lips is examined and the succesions of decohesion mechanims is deduced. The aproximate change of fracturing temperature due to adiabatic dissipation of deformation energy as heat is deduced, also.

Key words: Charpy test, structural steels, ductile fracturing, load-deflection dependence, consumption of energy, fracture surface and lips

Proces Charpy prijeloma u duktilnom području. Izražen je proces Charpy prijeloma u duktilnom području. Određene su ovisnosti sila-savijanja i sila-vrijeme te potrošnja energije za različite faze prijeloma, npr. plastično savijanje i propagacija pukotine. Ispitna je mikromorfologija površine prijeloma i određen je redosljed mehanizama dekohezije. Izračunata je promjena temperature prijeloma glede adiabatske pretvorbe deformacijske energije u toplinu.

Ključne riječi: Charpy test, konstrukcijski čelik, duktilni prijelom, ovisnost sila savijanja, potrošnja energije, površina i presjek prijeloma

INTRODUCTION

Charpy (CVN) toughness tests are videly used to determine the effect of temperature on the propensity of structural steels to brittle fracture. Notched specimens are submitted to the impact of a hammer with the kinetic energy of 300 J. The fracturing occurs in ductile, mixed or brittle mode and, accordingly, a very different quantity of energy is consumed. Generally, in the upper shelf CVN ductile region, the energy consumed for the fracture of structural steels is 150 J and more and it is different for different steels. The energy consumed for brittle cleavage fracture below the lower shelf threshold is below 10 J and very similar for steels with different microstructure, a wide range of grain size and yield stress as well as for as delivered and strain aged steels [1] (Figure 1).

The fracturing time depends on the fracturing energy and it is very different, it is of 11 ms with the energy of 250 J and of 1 ms with the energy of below 10 J.

Also the volume of the plastically deformed metal is very different, it amounts to several hundreds of mm^3 in the ductile range and it is negligible in the brittle range [2]. Virtually 90 % of the energy consumed for the plastic deformation and fracturing is dissipated as heat [2, 3]. For this reason, the fracturing in the upper shelf and transition range occurs above the nominal testing temperature.

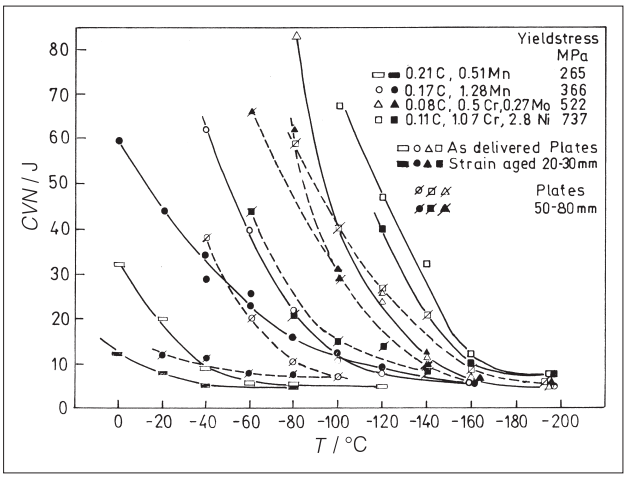

Figure 1. Charpy notch toughness for structural steels with different microstructure and yield stress in the range of transition temperature [1]

In brittle range virtually no plastic deformation heat is generated and the fracturing occurs at the nominal testing temperature [1]. Therefore, the temperature, which is used to show graphically the dependence CVN toughness versus testing temperature, is not the real fracturing temperature for the vhole testing interval. The time and volume distribution of deformation and fracturing temperature complicate additionally the proper understanding of the Charpy ductile fracturing mechanism.

F. Vodopivec, B. Arzenšek, J. Vojvodič Tuma, R. Celin, Institute of metals and Technology, Ljubljana, Slovenia

Let us quote some opinions on the different events involved in the CVN fracturing process. It is stated [4] that the Charpy tests consist of a variety of cumulative events and that several events in the fracturing zone are competitive in terms of local stress and strain. The Charpy specimen is to small to develop a steady state fracture mode [5]. The sensitivity to brittle fracture depends on the tip radius [6, 7]. The cleavage fracture is initiated with a ductile mode propagating crack when the tensile stress exceeds a critical stress on a certain microstructurally determined distance ahead the crack tip [8]. The change from ductile to brittle crack propagation mode occurs after plastic slip ahead the ductile crack tip [9, 10]. The critical COD and crack tip radius size were calculated for the fracture mode change [10]. The energy absorbed for the fracture depends on the amount of plastic deformation prior to crack initiation and multiple activation of crack sources takes place [11]. Mixed mode fracture energy is increased by a factor of two if the crack inclination angle is decreased from 90° to 60° toward the specimen axis by tests at liquid nitrogen temperature, while at room temperature this angle has no effect on the fracture energy [12]. The combined criterion for cleavage fracture consists of a critical plastic strain for the initiation of the crack nucleus, a critical stress triaxiality for preventing its blunting and a critical normal stress for its propagation [13]. By reducing the notch tip radius of a CVN specimen, the stress concentration at the crack tip is increased [14]. Three caracteristical points: the yield, the maximal stress and the point of crack initiation are found on the Charpy load versus time signal [15]. On brittle fracture river patterns are found on (110) cleavage facets, while the (100) facets are smooth [16]. The cleavage fracture strength is a temperature [17, 18] and grain size [8, 19] dependent steel property of notched CVN specimen. The stress concentration factor (K_p), ratio of the stress intensity in notched specimen, is calculated as [20]:

$$K_p = 1 + \ln(1 + R / r) \qquad (1)$$

With R – size of the plastic zone ahead the notch tip and r – notch tip radius (r = 0,2 mm for the CVN specimen).

These short quotations from selected references shows that some events of the Charpy fracturing process are well understood, while the fracturing process, as the joining of these events was not yet explained. In this article the results of tests performed with the aim to determine a comprehensive explanation of the follow up of the Charpy ductile fracturing events and the energy related are presented and discussed.

EXPERIMENTAL WORK

The tests were performed with two structural steels: steel A with a microstructure of ferrite and pearlite with the linear intercept grain size of about 3,5 μm and the yield stress of 512 MPa and steel B with a microstructure of polygonal ferrite and pearlite with linear intercept length of 35 μm and yield stress of 362 MPa. For both steels the maximal upper shelf energy was of about 260 J, the transition temperature were of -105 °C for the steel A and -81 °C for the steel B. Tests on standard CVN specimens were performed on an instrumented Charpy hammer with computer recording of the load (deflection force) versus specimen deflection (Figure 2) and load versus the test time.

The recorded dependences load versus deflection and load versus time were of essentially similar shape. For this reason, in this work only data from the dependence flexion force versus deflection are used. The time span of recordimg steps was of 10 μs and the deformation and fracturing time was of 10 ms for ductile range, of 2 to 3 ms for the mixed ductile brittle fracture and below 1,5 ms for brittle fracturing [1]. Two parallel tests were performed for every temperature in the range in the upper to in the lower shelf notch toughness. Of all data, in this work only the results of tests of fracture in upper shelf range are reported and discussed.

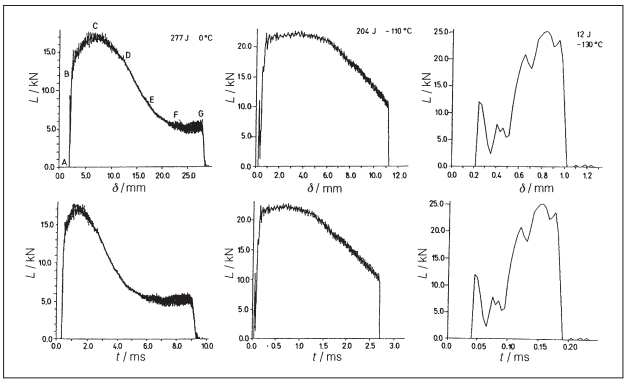

Figure 2. Examples of recording deflection force versus deflection and versus time for Charpy test in ductile, transition and brittle temperature ran-

The different deformation and fracturing events were established as charateristic points of the relationshipt deflection force versus deflection (df-d) that was used also for acquiring quantitative data on the deflection, force and consumed energy (Figure 3). This energy was determined with planimetry of segments obtained with vertical projection of characteristic points of the (df-d) curve on the abscissa. The yield stress and maximal stress obtained from (df-d) curves was compared to tensile properties assuming that because of the very small deflection angle up to the start of plastic deformation, the Charpy specimen was a beam with the shape of the notched CVN specimen.

The temperature in the specimen was deduced for specific points of the (df–d) curve assuming that the plastic deformation energy (CVN) was dissipated as adiabatic heat [3, 21] in the deformed volume of metal using the relation:

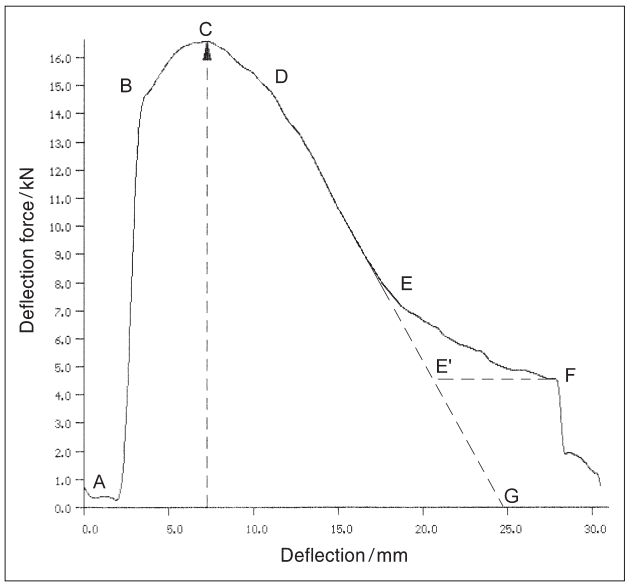

Figure 3. Dependence deflection force versus deflection fo the Charpy nocth toughness test in upper shelf range with marked the different events

$$\Delta T = 0{,}90 \cdot (CVN) / V \cdot c \cdot p \qquad (2)$$

With T – temperature in °C, V – volume of the deformed metal, c – specific heat of the metal (for steel c = 44,8 J/N °C, p – specific density (for steel P = 7,86 10^4 N/m^3.

The volume of deformed metal was determined considering the difference of the initial specimen shape and its shape after cracking and ejection assuming that the change of shape was in form of a triangular prism with as base the thickness of the specimen and as height the distance of the point of maximal striction and the point on the lateral surface, where the it was possible to discern the change of straigthness.

Theorically, the hammer of mass 20kp (w) impacts the specimen back side (side opposite to the notch) with the kinetic energy of 300 J with the speed of v=5,36 ms^{-1}, which corresponds to the initial deflection rate. The hammer kinetic energy is consumed in the deflection of the specimen and the hammer speed is lowered in dependence of the consumed energy (CVN). After a determined quantity of energy is consumed, the hammer kinetic energy is related to its initial energy as [10]:

$$(w \cdot c^2 / 2 \cdot g) = 300 - CVN$$

And the velocity is deduced as:

$$c = 0{,}31 \cdot (300 - CVN)^{1/2} \qquad (3)$$

The hammer impact produces a strong plastic deformation in a layer of steel at the specimen backside (Figure 4). In the specimen of steel A the initial HV hardness of 160 was increased to 340 expected after an absolute plastic deformation of 0,82 [22], or a relative deformation of above 80 %. The width of the deformed layer is not uniform. On the longitudinal section of the specimen the deformed layer is in form of an envelope around the rounded tip of the hammer with the width gradually diminishing to a distance of about 10 mm from the point of impact. It was assumed that the back side deformation of the specimen is ocurring for the must of the deformation and fracturing time of the specimen and it is recorded in the relationship flexion force versus deflection.

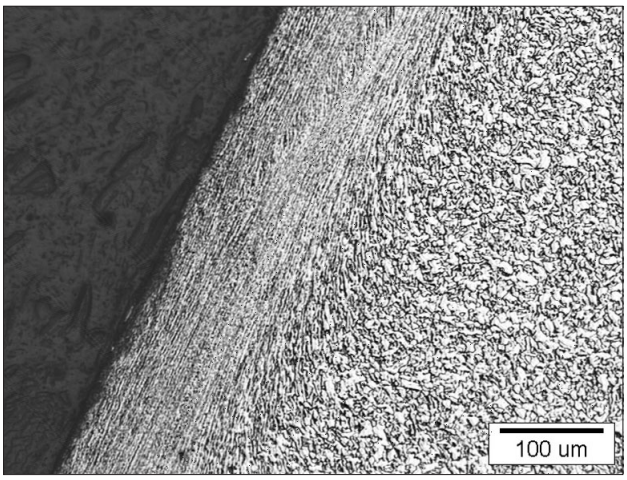

Figure 4. Layer of plastically deformed steel backside of the specimen in the area of hammer impact

CONSUMPTION OF ENERGY FOR THE FRACTURING EVENTS

After the hammer impacts the specimen (point a in Figure 3), the deflection force (df) increases proportionally to the deflection (d) up to point B, where the plastic deformation starts. In the segment A-B the deformation of the specimen is elastic. The deflection force than increases from point B to its maximal value at the point C approximately parabolically with the deflection, thus DF ≈ f($d^{1/2}$) [23] (Figure 5).

At the point C, where the crack was initiated [15], the deflections were on average of 4,03 mm for steel A and of 4,34 mm for steel B for testing at 0 °C and the specimen angle of 11° toward the initial plane. At lower testing temperature the deflection at the point C was

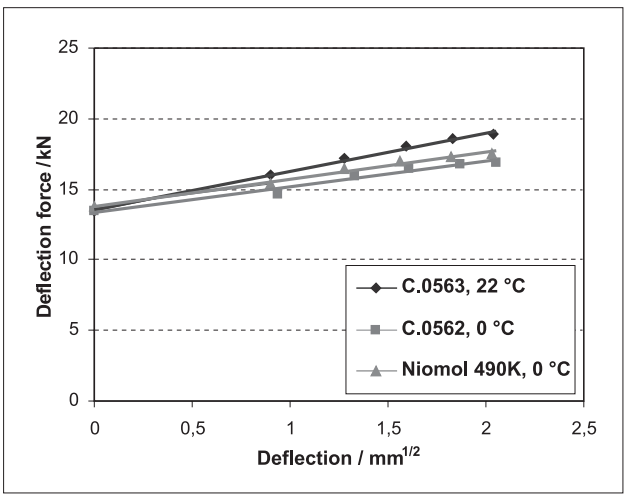

Figure 5. Increase of the deflection force in the B – C part of the (df-d) curve versus the square root of deflection

smaller. Of side the point C, the crack length increases and the ligament length and the volume of plastic deformation decrease, parallely the deflection force decreases to the point D. The shape of the segment C-D of the (df–d) curve is similar as in the B–C segment and it confirms the equality of the deformation process both sides of the point C. The decrease of the deflection force in the C–D segment of the curve is explained with the decreasing volume of deformation due to the decrease of the ligament thickness. Of side the point D the deflection force decreases to point E proportionally to the deflection and to the decrease of the ligament thickness. On some specimens a slight bulge in this part of the (df-d) curve was recorded, indicating probably a slight deviation of the crack extension plane from the notch tip plane. The proportionality stops at the point E and beyond this point, than the deflection starts to increase faster than the crack extension rate because the specimen is pushed in between the supports to the point F, where the unfractured specimens is ejected. In absence of the part E-F of the (df-d) curve the fracturing would proceed theoretically according to the prolongation of the proportionality D-G' to the specimen back side. It is possible to calculate the length of crack extension at any point of the segment C–E assuming that the ductile fracturing would reach the specimen back side on the point G. At the point E the specimen is bent for 15 mm and with respect to the initial plane, the bending angle is of aproximately 37°. At ejection, the bending angle of the specimen is approximately of 55°.

The initial hammer rate of 5,36 ms^{-1} decreases with the consumption of energy and can be deduced from equation (3). It is f.i. of 4,58 ms^{-1}at the point C, of 3,63 ms^{-1} at the point D and of 1.96 ms^{-1} at the initial of pushing the specimen between its supports at the point E. The linearity of the segment C-E of the (df–d) curve is explained asuming that in this segment the crack extension rate is equal to the deflection rate.

The energy consumed for different deflection and fracturing events was determined with planimetry of the area of the geometrical figure given by the projection of the length of different segments of the (df–d) curve on the abscissa and the energy consumed by the friction at pushing the specimen in betweem its supports by planimetry of the area E-E'-F. The obtained share of energy for different events are given in Table 2.

The share of energy spent for the initial elastic deflection is sligthty higher for specimens of the steel A with higher yield stress. Above half of the total energy is consumed in the evencts involving the plastic deformation in absence and in presence of a crack of length up to approximately 2 mm when the linear crack extension is started.

In terms of consumption of energy for different Charpy events, no systematical difference is found for both steels with exception of the energy consumed in the pushing of the specimen between its supports, which is higher for the steel A. For both steels the energy consumed for those two events is higher at lower testing temperature.

At the point B the yield stress is achieved for bending the CVN specimen. At this point, the deflection is of approximately 0,65 mm [23]. The ratio of bending and tensile yield stress calculated assuming the specimen to be a centrally loaded beam, was of K_p = 2,42 to 2,63 for the steel A and higher, K_p = 3,22 to 3,35 for the steel B. In the segment B–C of the (df-d) curve the deflection force increases as the quare root of the deflection (Figure 5) and shows a sligthly stronger strain hardening for the steel A. It is, thus, possible that the difference in notch sensitivity is related to the strain hardening, which may affect the size of the plastic zone ahead the notch tip. For both steels and room temperature, the radius of the plastic zone R deduced applying the relation (1) and considering the experimental value of K_p and the notch radius r = 0,0025 m was greater than the specimen width.

The deflection force in the segment D-E of the (df-d) curve decreases proportionally to the deflection, to the increase of the crack extension and with the decrease of the ligament section. In this segment the deflection force is the sum of the deformation force, which decreases with the decrease of the ligament section and of the crack opening force, which is assumed to be constant.

Table 2. **Consumption of energy for different events and maximal deflection force for Charpy tests of steels A and B in ductile fracturing range [23]**

Segment			A-B	B-C	C-D	D-G	Push	Sp. Ben.	CVN	Def. Force / kN
Steel A	-60 °C	J	7,2	76,0	70,9	59,9	18,2	25,8	258,3	18,3
		%	2,8	29,4	27,4	23,1	7,0	9,9		
	-20 °C	J	6,3	68,2	85,5	48,0	9,8	31,0	258,4	17,8
		%	2,5	27,3	34,3	18,6	3,8	11,9		
Steel B	-20 °C	J	6,0	64,3	86,9	58,8	19,2	20,8	257,8	18,0
		%	2,3	26,9	34,1	22,8	7,4	8,1		
	20 °C	J	5,9	74,9	104,9	59,1	12,2	8,5	264,8	19,1
		%	2,2	28,1	39,6	27,3	4,6	3,2		

A-B - elastic deflection, B-C - deflection with plastic deformation, C-D - deflection with plastic deformation and crack propagation, D-G - theoretical crack extension to complete fracture of the specimen, Push.- energy spent for friction between the specimen supports and the E-E' crack extension, Sp. ben. - energy spent for the bending of the ejected unfractured specimen; CVN - Charpy energy.

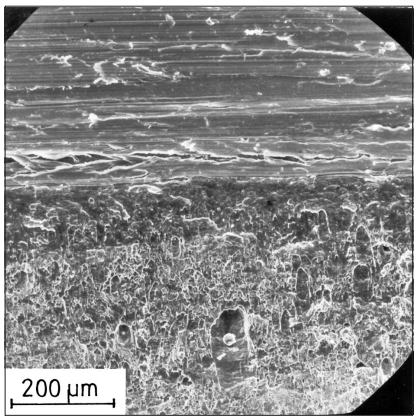

Figure 6. Fracture surface at the notch tip

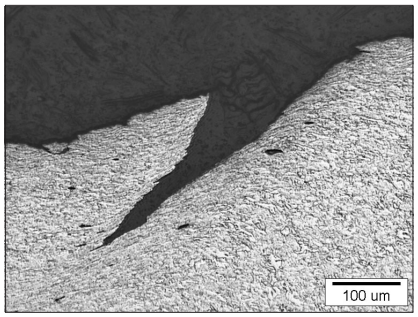

Figure 7. Micrography. Section of the main and the secondary crack at the notch tip

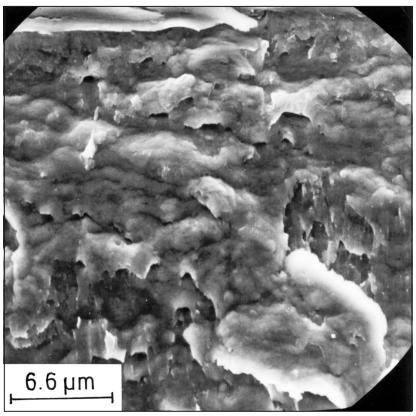

Figure 8. Micromorphology of the fracture surface in the flat band along the notch tip in Figure 7

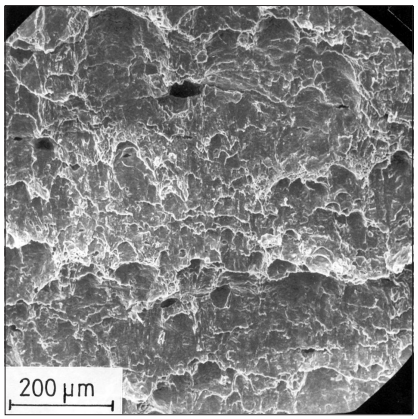

Figure 9. Fracture surface at greater distance of the notch tip

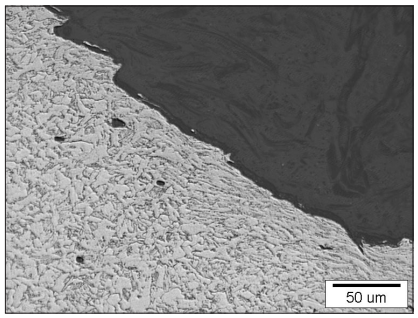

Figure 10. Micrography. Section of the fracture surface lip with shear deformation preceeding the decohesion

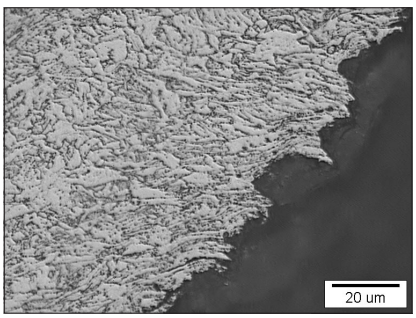

Figure 11. Micrography. Section of the fracture surface with normal deformation preceeding the decohesion

For specimens with crack extension in the notch tip plane the average value of crack opening force of 67,5 N was deduced assuming the crack width is equal to the width of the specimen. The deformation force generates a complex stressing in the crack extension plane of the ligament, as the bending of the specimen generates pressure stressing in half and tensile stressing in the other half of the ligament with zero stressing in the neutral axis. For all specimens with crack extension in the notch tip plane an average stressing of 27,6 MPa was deduced, a value which combines both types of stressing and reflects the stressing triaxiality.

MORPHOLOGY OF THE CRACK SURFACE AND SECTION

The examination of the fracture surface and of the crack section, which showed the morphology of the crack lips and the extent of cold deformation in their vicinity, was performed only for specimens of the steel A. At visual examination several cracks initials in the notch tip (Figure 6) were observed, as reported allready [10, 13]. On the profile of the fracture surface it is evident that the propagation was arrested for the cracks propagating outside the notch plane of maximal stress (Figure 7). Several initial cracks were found also on notched tensile specimens tested in brittle fracture range [22]. No evidence of parallel crack initiation was found on the (df-d) curves and it is concluded that the initiation of all cracks in the specimen notch was virtually simultaneus. The squeezed shape of grains along the lips of the main and the secondary crack indicates to a strongly localised shear deformation preceeding the crack opening. In the flat fracture band near the notch tip only rare and small dimples were found. Their shape and orientation in the direction of crack propagation confirm additionally the shearing process of decohesion. Further on the fracture surface, areas with flattened dimples alternated to areas of normal propagation (Figure 8 and 9) were found. Accordingly, on the fracture lip segmemts with strongly localised shearing deformation and normal decohesion were observed (Figure 10 and 11).

DISTRIBUTION OF PLASTIC STRAINING AND FRACTURING TEMPERATURE

Near the crack lips the deformed and unfractured or fractured specimen has a complex shape. In the notch tip plane the width of the specimen is not changed. At the distance of 3,2 mm from the notch tip, the width is di-

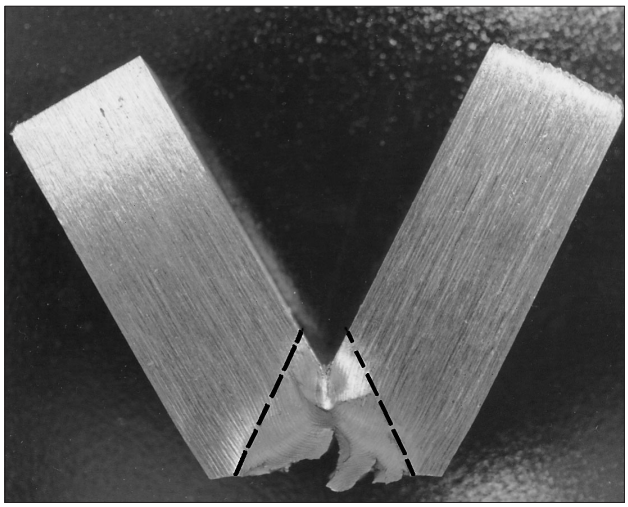

Figure 12. Unfractured specimen ejected from the Charpy device with marked the aproximate area of plastic deformation

minished to 7,9 mm and on the back side it is increased to 11,9 mm (Figure 13). On the lateral side two rounded areas of plastic deformation are distinguished, one along the crack lips with the apex in the notch tip and the second at the compressed specimen back side with greater intensity of plastic deformation in the area of contact of specimen halfs. On both lateral surfaces the limit of plastic deformation is clearly marked as outset of curving of the planing scratches. The width of the zone of plastic deformation on the back side of the specimen was of 6,2 mm. The zone of plastic deformation was, as marked in Figure 12, on the lateral surface aproximated with a triangle with the apex in the notch tip. In was assumed that the deformation volume is a triangular prism with the base plane of (6,4 × 12) mm on the specimen backside and with the apex on top of the ligament. For the point C the ligament thickness is of 8 mm and equal to the specimen thickness. For the point B the initial thickness was diminished for half of the crack propagation between points C and D of the (df-d) curve (crack length 3,36 mm, ligament 6,32 mm) and for the point E for the length of crack propagation between the point C to half of the distance D-E (crack length 4,56 mm, ligament 3,44 mm).

The deformation and fracturing time is only of 11 ms and the adiabatically generated heat does not diffuse from the volume of generation.

For the calculation of the deformation and crack propagation temperature the average of data data acquired from two specimens of steel B tested at room temperature were used considering the prismatic volume of plastic deformation of $3{,}07\times10^{-7}$ m^3, for the point D of $2{,}42\times10^{-7}$ m^3 and for the point E of $1{,}32\times10^{-7}$ m^3 and the consumption of energy of 74,6 J at the point C, of 104,9 J at the point D and of 43,7 J at the point E.

Of the total consumed energy of 264,8 J, thus 84,3 % was considered in the calculation, the difference to 100 % is the sum of energy for the initial elastic deformation, for the final elastic bending and for the friction of the

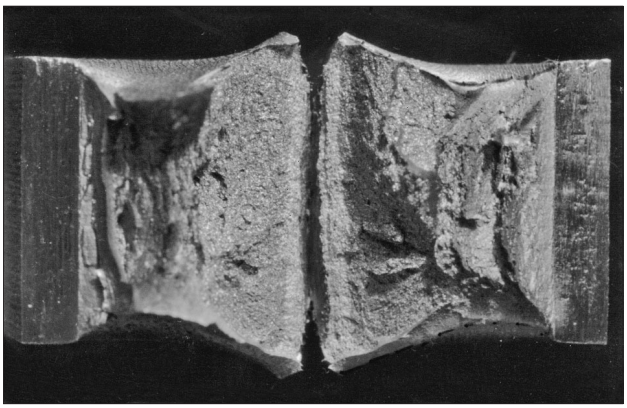

Figure 13. Fracture surface of a Charpy specimen broken after ejection

specimen against the supports. These shares of consumed energy do not affect the generation of heat in the volume of deformation and crack propagation.

Introducing in equation (2) the quoted data the following increases of temperature are obtained: for the point C 62,6 °C, (62,6+111,6)=174,2 °C for the point D and (174,2+85,2)=259 °C for the point E.

At every point the temperature is higher for the testing temperature of 20 °C. The calculated temperature for the point E was of 279 °C. The change of shape of the specimen near the fracturing surface and the microstructure indicate that the distribution of plastic strain is not uniform over the prismatic deformation volume and that the maximal deformation intensity is achieved at the fracture surface. Assuming a linear distribution of deformation intensity over the deformation volume with the maximum at the area of greatest microscopic deformation, the temperature increase in this area was twice of that deduced for the uniform distribution of deformation intensity, thus of (518 + 20) = 538 °C.

As shown in Figure 7, 10 and 11 in microscopic scale, the deformation intensity is much greater in a very narrow layer of steel near the fracture surface, than at the distance of a few ten of μm. The great difference in deformation intensity over the small distance, which is also the indication for a strong temperature gradient, can be explained assuming that the increased temperature produced the lowering of the steel compression strength at the fracture surface and a high temperature gradient over a distance of few ten of μm. It is possible even that the temperature was sufficiently high for dynamic recovery to occur and dimisnish the strain hardening in the linear C–D part of the (df-d) curve. A high temperature in the crack propagating layer would also explain the low value deduced for the crack opening force.

CONCLUSIONS

Notch toughness tests were performed on two structural steels with different microstructure and yield stress and similar Charpy toughness in ductile range with the aim to investigate the dynamics and the mechanism of

fracturing in upper shelf range. The tests were performed on an instrumented Charpy device with load and deflection measured in intervals of 10 μs. The microstructure was investigated with optical microscopy and the fracture surface was examined with scanning microscopy. Based on the results of the investigation and the findings in the quoted references the following conclusions are proposed:

- it is confirmed that several cracks are initiated in the notch tip and the crack in the notch plane becames propagating;
- all events of the deformation and cracking of the CVN specimen submitted to the Charpy test: elastic and plastic bending deformation, strain hardening, crack initiation and crack propagation are clearly distinguished on the curve deflection force versus deflection, although the deformation and crack growth time was of about 11 ms;
- the fracture surface and section show that the crack is opened with shear deformation and the the propagationn occurs with alternated shearing and normal decohesion areas;
- the share of energy for the different events: elastic deformation, plastic deformation and plastic deformation and crack extension is similar for both tested steels and it is not related to the difference in yield stress of both steels;
- the yield stress is and the intensisty of strain hardening are lower for the steel B. As the maximal deflection force is very similar for both steels, it is assumed that the deformation volume is greater for steel B with lower yield stress;
- parts of the total consumed energy are consumed also for secondary events. In the range of testing temperature 22 °C to -60 °C the share for the initial elastic deformation was of 2,2 to 2,8 %, for the friction at the pushing of the unfractured specimens between its supports of 3,8 to 7 % and for the elastic bending of the unfractured specimen of 3 to 12 %.
- the adiabatic dissipation of deformation energy to heat increases significantly the temperature in the deformation and fracturing volume of steel. In a thin layer of metal near the fracture surface the steel temperature may have been risen to the level of significant decrease of the steel shear strength. The temperature gradient is very strong near the tip of the propagating crack. It is even possible that the increased temperature is sufficient for dynamical recovery to decrease the strain hardening in the D–E part of the (df-d) curve.

REFERENCES

[1] F. Vodopivec and J. Vojvodič-Tuma, Proc. Int. Symposium" Mechanical Properties of Advanced Engineering Materials", 27-31 May 2001, Mie Un., Japan.

[2] F. Vodopivec, B. Breskvar, J. Vojvodič-Tuma and D. Kmetič: Kovine Zlitine Technologije (Metals Alloys Technology), 33(1999), 393-400.

[3] W. Dahl and H. Rees: "Grundlagen des Festigkeits und Bruchverhalten", 54-70, 1974, Verlag Stahleisen, Düsseldorf.

[4] J. Lerein and J.D. Embury: Conf. Proc. "What the Charpy tests show us", Denver, CO, 27-28 Nov. 1978, 33-53, Mater. Park, OH, ASM International.

[5] G.M. Wilkowski, W.A. Maxey and R. J. Eiber: Ibidem 108-132.

[6] C.E. Harbower and R.D. Sumbury: Ibidem, 151-171.

[7] T. Miyata, A. Otsuka, M. Mitsubayashi, T. Haze and S. Aihara: "Fracture Mechanics 21th. Symposium", 1990, ASTM, Philad., STP 1074, 361-377.

[8] D.A. Curry: Met. Sci., 14(1980), 319-326.

[9] P. Brozzo, M. Capurro and E. Stagno: Mater. Sci. Technol., 10(1994), 334

[10] F. Vodopivec, B, Breskvar, B. Arzenšek, D. Kmetič and J. Vojvodič-Tuma: Mater. Sci. Techn., 17(2001), 1-7.

[11] M. Naguno and Y. Sawano: J. Japan Inst. Metals, 54(1990), 420-426.

[12] B.H.J. Koch, C.A. Kwa and M. Manoharan: Inter. J. Fracture, 77(1996), R77-R81.

[13] J.H. Chen, G.Z. Wang, C. Yan, H. Ma, L. Zhu: Inter. J. Fracture, 83(1997), 121-138.

[14] S. Mikalac, M.G. Vassilaros, H.C. Rogers: Int. Conf. "Charpy Impact Tests: Factors and Variables", Lake Buena Vista FLO, 1990, ASTM STP 1072, Phil., 134-141.

[15] D. Pachura: 16th Intern. Conf. On Effects of Radiation on Materials, 23-25 june 1992, Aurora,CO, ASTM STP 1175, 1994, 195-210.

[16] S.T. Mandziej: Metall. Trans. A, 24 A(1993) 545-552.

[17] C. Jüde-Esser, F. Grimpe, W. Dahl: Steel Res., 66(1995) 259-263.

[18] D.A. Curry and J.F. Knott: Met. Sci., 10(1976), 1-6.

[19] R. Sandström and Y. Bergsström: Met. Sci., 18(1984), 177-186.

[20]]H. Kurishita, H. Nayano, M. Narui, M. Yamazaki, Y Kano, I. Shibahara: Mater. Trans., JIM, 34(1993), 1042-1052.

[21] R.J. Hand, S.R. Foster and C.M. Sellars: Mat. Sci. Techn. (2000)16, 442.

[22] G. Kosec, dr. thesis submitted to Un. of Ljubljana, november 2007.

[23] F. Vodopivec, B,. Arzenšek, D. Kmetič, J. Vojvodič-Tuma: Materiali in Tehnologije 37(2003), 217.

Note: The responsible translator for English language is mr. Franc Vodopivec.